Proc. Natl. Acad. Sci. USA
Vol. 92, pp. 3488–3492, April 1995
Medical Sciences

Cell cycle-related shifts in subcellular localization of BCR: Association with mitotic chromosomes and with heterochromatin

(*BCR/ABL/BCR-ABL*/leukemia)

MEIR WETZLER*†, MOSHE TALPAZ‡§, GARLAND YEE¶, SANFORD A. STASS‖, RICHARD A. VAN ETTEN**, MICHAEL ANDREEFF§, ANGELA M. GOODACRE§, HANS-DIETER KLEINE§, RADHA K. MAHADEVIA§, AND RAZELLE KURZROCK†‡§

*Department of Medicine, Roswell Park Cancer Institute, Buffalo, NY 14263; Departments of ‡Clinical Investigation, §Hematology, and ¶Laboratory Medicine, University of Texas M.D. Anderson Cancer Center, Houston, TX 77030; ‖Department of Pathology, University of Maryland Medical System, Baltimore, MD 21201; and **Center for Blood Research, Boston, MA 02115

Communicated by Peter C. Nowell, University of Pennsylvania School of Medicine, Philadelphia, PA, December 20, 1994

ABSTRACT **The disruption of the *BCR* gene and its juxtaposition to and consequent activation of the *ABL* gene has been implicated as the critical molecular defect in Philadelphia chromosome-positive leukemias. The normal BCR protein is a multifunctional molecule with domains that suggest its participation in phosphokinase and GTP-binding pathways. Taken together with its localization to the cytoplasm of uncycled cells, it is therefore presumed to be involved in cytoplasmic signaling. By performing a double aphidicolin block for cell cycle synchronization, we currently demonstrate that the subcellular localization of BCR shifts from being largely cytoplasmic in interphase cells to being predominantly perichromosomal in mitosis. Furthermore, with the use of immunogold labeling and electron microscopy, association of BCR with DNA, in particular heterochromatin, can be demonstrated even in quiescent cells. Results were similar in cell lines of lymphoid or myeloid origin. These observations suggest a role for BCR in the phosphokinase interactions linked to condensed chromatin, a network previously implicated in cell cycle regulation.**

The *BCR* gene plays a crucial role in the pathogenesis of leukemias bearing the Philadelphia (Ph) translocation [t(9;22)(q34;q11)] (1). Juxtaposition of the *BCR* and *ABL* genes in these leukemias results in the formation of their molecular hallmark—a chimeric *BCR-ABL* gene (2–4). The BCR-ABL fusion protein is capable of inducing chronic myelogenous leukemia (CML)- or acute lymphoblastic leukemia (ALL)-like diseases in mice and can transform lymphoid cells and some types of fibroblasts *in vitro* and, therefore, is believed to be critical to the oncogenic process (5, 6); its transforming ability is related to the activation of the tyrosine kinase enzymatic activity and the actin filament-binding function of ABL by BCR sequences (7–9).

Although the role of the normal BCR product in hematopoiesis remains unclear, several functional domains have now been defined for this protein (10), and it has been implicated at many levels in the two major intracellular signaling mechanisms in eukaryotic cells (phosphorylation and GTP-binding). The first exon [which is the region critical to activating the transforming function of BCR-ABL (10)] encodes a structurally novel serine/threonine-protein kinase domain (11, 12). Central BCR sequences show homology to the *cdc24* gene (a cell division cycle control gene involved in cytoskeletal organization and the regulation of budding in yeast) and its probable human homologue, the protooncogene *DBL* (13, 14). The C terminus of BCR has homology to a prototype GTPase-activating protein (GAP) for the RAS-related rho GTPases and has GAP activity for the $p21^{RAC}$ and the CDC42Hs members of the RAS superfamily of GTP-binding proteins (15–17). The above activities are consistent with the immunocytochemistry-based localization of the BCR protein to the cytoplasm in uncycled cells (18, 19). Our current results demonstrate, however, that the BCR protein adopts a predominantly perichromosomal position in mitotic cells and further that, even in interphase cells, association of BCR with chromatin can be discerned by immunoelectron microscopy.

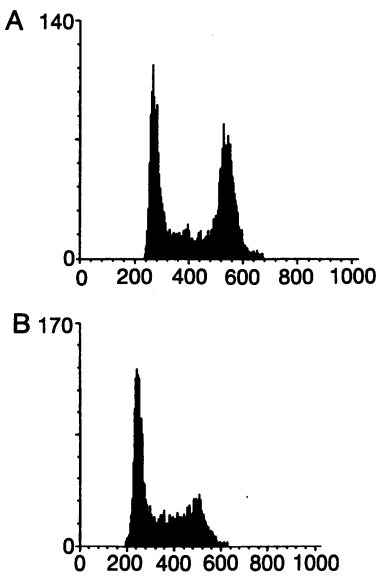

FIG. 1. DNA content of HL-60 cells. Cells were harvested and stained for DNA with acridine orange as described in *Materials and Methods.* (The *x* axis of the graph represents the DNA content as reflected by fluorescence intensity; the *y* axis is the number of cells per channel.) (*A*) Cells released from double aphidicolin block. (*B*) Control cells. Peaks: 1, DNA content at $G_{1/0}$; 2, DNA content at G_2/M. The interval between the peaks shows the DNA content at S phase.

MATERIALS AND METHODS

Cell Lines. We used the promyelocytic leukemia cell line HL-60, the acute monocytic leukemia cell line THP-1, the acute myelogenous leukemia cell line KG-1, and the Burkitt lymphoma cell line Daudi (all obtained from the American Type Culture Collection).

The publication costs of this article were defrayed in part by page charge payment. This article must therefore be hereby marked "*advertisement*" in accordance with 18 U.S.C. §1734 solely to indicate this fact.

†To whom reprint requests should be addressed at: Department of Clinical Investigation, Box 302, M.D. Anderson Cancer Center, 1515 Holcombe Boulevard, Houston, TX 77030 (R.K.) or Roswell Park Cancer Institute, Elm and Carlton Streets, Buffalo, NY 14263 (M.W.).

Cell Cycle Synchronization. Synchronization at the G_1/S boundary was achieved with aphidicolin block (20). Cells at 5×10^5 per ml were blocked with 5 μg of aphidicolin per ml for the length of their doubling time and released from the block by three washes in fresh medium. This process was repeated, and the cells were allowed to recover for the length of their S phase before harvesting for analysis. To verify that the cycled cells had been enriched for the G_2/M population, DNA content was analyzed by staining DNA with acridine orange (Polysciences) (1.0 mg/ml) and analyzing immediately with FACScan (Becton Dickinson) and Lysis II software (Becton Dickinson).

Cell Sorting. Flow cytometric analysis and cell sorting were performed with the FACS Vantage fluorescence-activated cell sorter (Becton Dickinson) with the Lysis II software. By using nuclear staining with Hoechst 33342 (Polysciences) (which stains DNA while preserving cell viability), gates were set to include cells at G_0/G_1, S, and G_2/M. Cells were collected for immunofluorescence and immunoelectron microscopy studies.

Antisera. For detection of the BCR protein, two antisera were used: (*i*) rabbit polyclonal sera against the β-galactosidase-BCR fusion protein (21), which was affinity-purified by using the glutathione *S*-transferase-BCR fusion protein; and (*ii*) monoclonal antibody 7C6 raised against the synthetic peptide bcr686 (Ser-Ser-Ile-Asn-Glu-Glu-Ile-Thr-Pro-Arg-Arg-Gln-Ser), originally described and characterized by Dhut *et al.* (18) (Oncogene Science). Control antibodies included a preimmune rabbit serum, an isotypic serum, and a monoclonal anti-human mitochondrial serum (Chemicon).

Immunofluorescence for Light and Confocal Microscopy. Immunofluorescence analysis by light and confocal microscopy was performed on paraformaldehyde-fixed cells by methods as described (19). [To better analyze mitotic cells (where indicated), swelling in 0.075 M KCl for 15 min at room temperature was carried out as an initial step.] Primary anti-BCR antibodies were used at a 1 (rabbit antiserum) or 2 (7C6 serum) μg/ml concentration, and incubations were 1 hr at room temperature. In all experiments rabbit preimmune serum or isotypic antibody were used as controls as appropriate for the antibody. In addition, where indicated, blocking of 7C6 serum with the cognate BCR peptide (10-fold excess by weight) was performed by preincubation. The appropriate secondary antibody (fluorescein isothiocyanate) for 7C6 serum and rhodamine for the rabbit antiserum; Jackson ImmunoResearch) was added at a 1:100 dilution for 30 min. Conventional epifluorescence microscopy was performed with an Olympus Vanox AH-2 fluorescence microscope. To specifically label the chromosomes, propidium iodide stain was included in the mounting medium (Imagenetics, Framingham, MA). For dual fluorescence, the Nikon Labophot-2 micro-

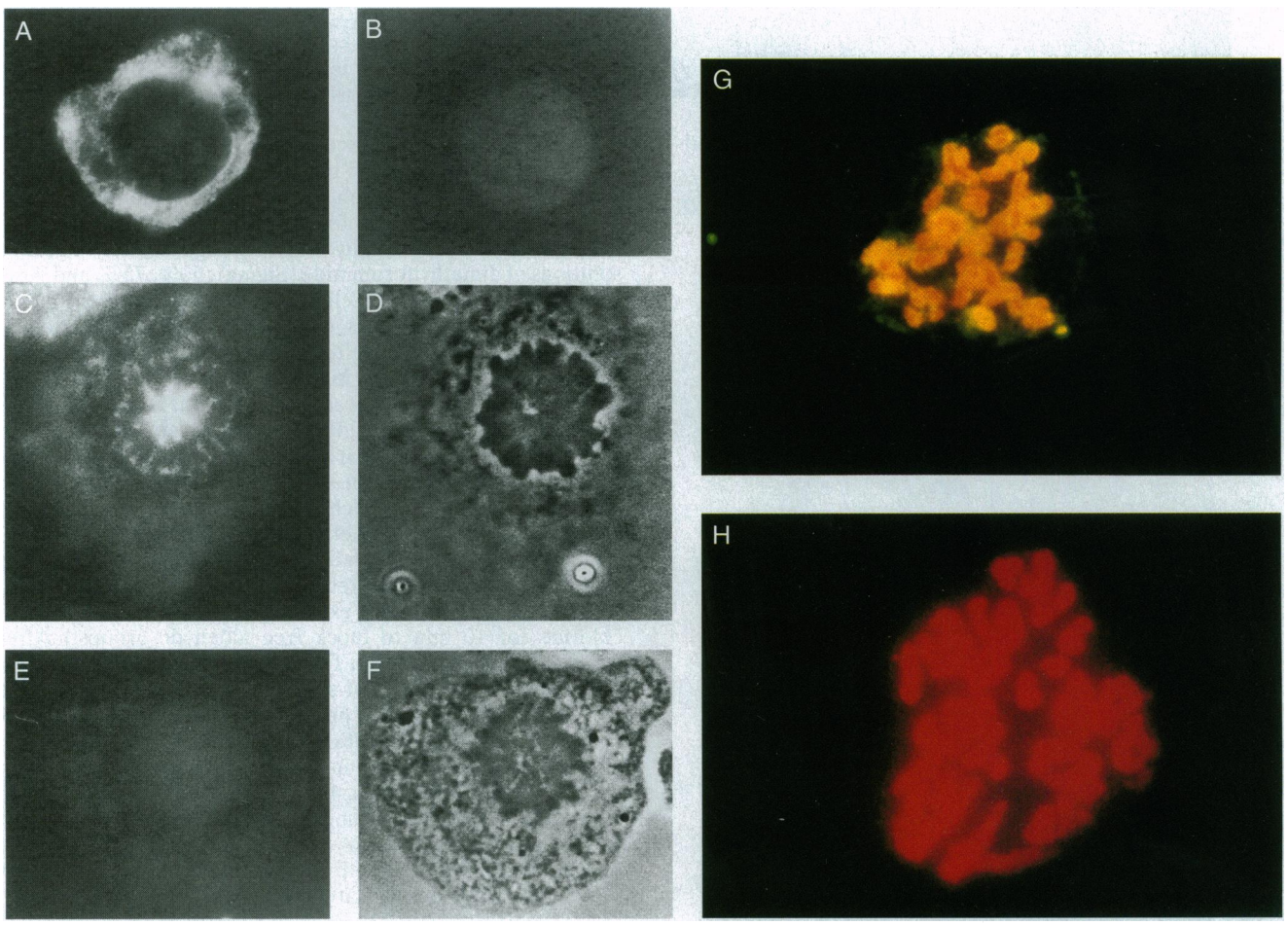

FIG. 2. Subcellular localization of BCR protein in interphase (*A* and *B*) and mitotic (*C–H*) KG-1 cells. The primary antibody was monoclonal anti-BCR (7C6) antibody. (*A*) Interphase cell exposed to the anti-BCR serum. (*B*) Interphase cell exposed to the primary anti-BCR serum blocked with cognate peptide. (*C*) Mitotic cell exposed to the anti-BCR serum. (*D*) Phase contrast micrograph of *C*. (*E*) Mitotic cell exposed to the primary anti-BCR serum blocked with cognate peptide. (*F*) Phase contrast micrograph of *E*. (*G* and *H*) Mitotic cells exposed to anti-BCR antiserum (*G*) and isotypic antibody (*H*). The mitotic cells were pretreated with 0.075 M KCl for 15 min at room temperature to swell the cells and better visualize the chromosomes. Mounting was performed in the presence of propidium iodide, and photography was done through double filters. Propidium iodide stains DNA red, whereas the fluorescein isothiocyanate-labeled primary antibody emits a green color, and the combination of red and green through the double filters appears yellow, indicating the association of BCR with chromosomal material. (*A–F*, ×730; *G* and *H*, ×440.)

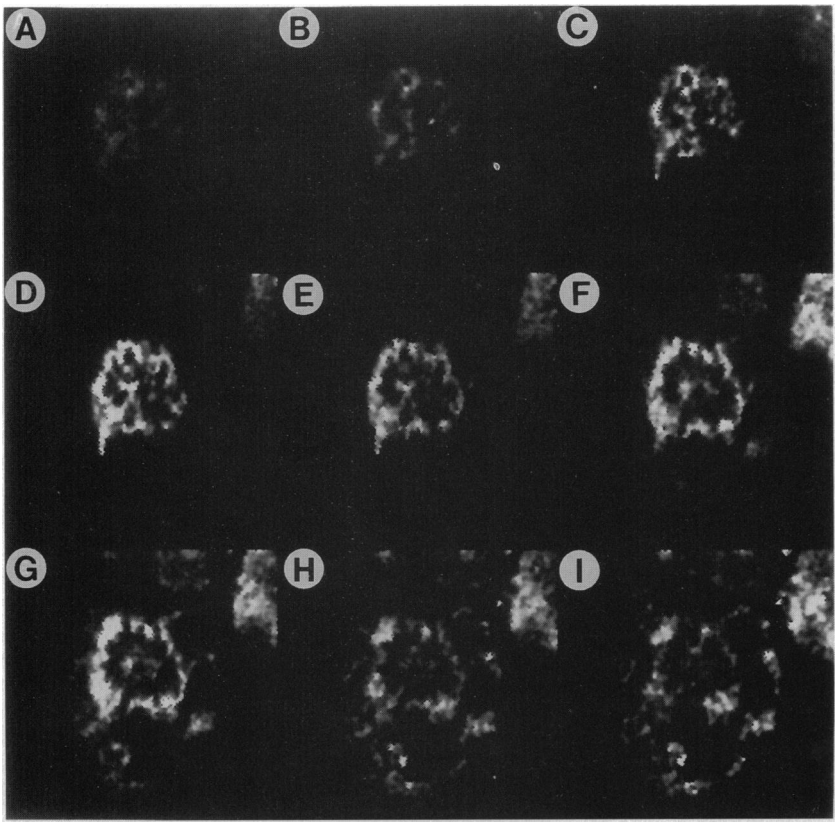

FIG. 3. Confocal laser-scanning microscopy of an HL-60 cell, demonstrating the association of BCR with the chromosomal surface in a mitotic cell. The primary antibody was monoclonal anti-BCR (7C6) serum. Scanning and data collection were performed on a Zeiss laser-scan microscope from the top (*A*) to the bottom (*I*) of the cell. (×360.)

scope was used. For three-dimensional imaging with confocal laser scanning, the Zeiss Laser scan microscope was used.

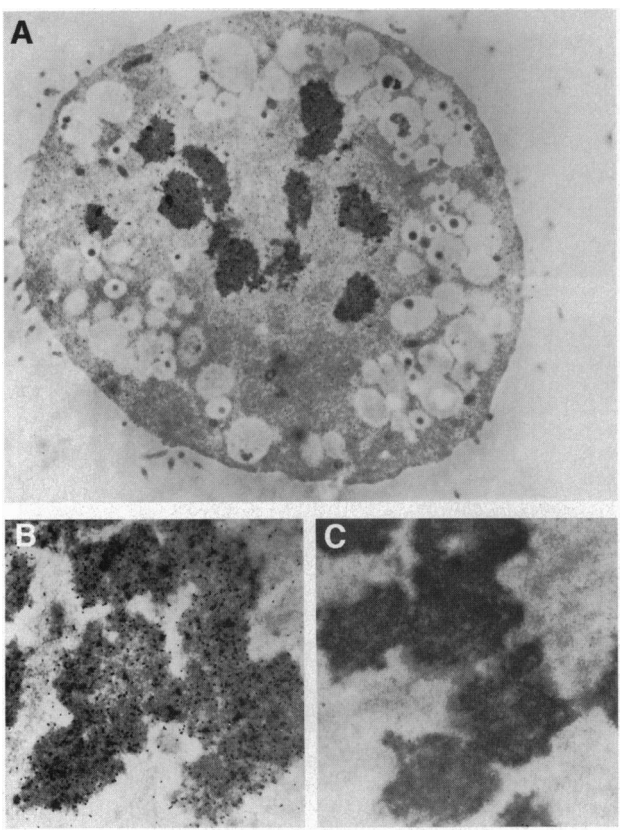

FIG. 4. Immunoelectron microscopy of mitotic HL-60 cells. The primary antibody was anti-BCR (7C6) serum. (*A*) Cell undergoing mitosis. (×2000.) (*B*) Higher magnification of a mitotic cell. (×6000.) (*C*) Exposure of a mitotic cell to the isotypic antibody. (×5000.)

Immunoelectron Microscopy. For electron microscopy examination, cells were fixed in either 2% glutaraldehyde (Sigma) or in 4% paraformaldehyde/0.1% glutaraldehyde in 0.1 M phosphate buffer (pH 7.3) for 1 hr at 4°C. After a rinse in the same buffer, cells were dehydrated through a series of graded solutions of dimethylformamide (Sigma) (50%, 75%, and 90%, vol/vol) in water at 0°C. Cells were then infiltrated through a series of graded solutions of Lowcryl K4M/dimethylformamide (Polysciences), 1:2, 1:1, and 2:1 (vol/vol), at 0°C and then incubated overnight in 100% Lowcryl K4M at −20°C. Polymerization at −20°C was brought about by indirect overnight ultraviolet irradiation. The blocks were irradiated for another 2- to 3-day period at room temperature to improve the sectioning properties. Thin sections (900 Å) were cut with a diamond knife on a Reichert Ultracut E microtome and mounted on Formvar nickel grids (Polysciences).

Immunolabeling for Electron Microscopy. Thin sections were floated on Tris-buffered saline (TBS) for 5 min. (In some cases, this was followed by exposure to TBS/0.5% ammonium chloride for 10 min to block free aldehyde groups.) After additional preincubation in TBS/0.1% bovine serum albumin/10% (vol/vol) normal goat serum for 15 min, the grids were kept overnight with the primary antibody [7C6 anti-BCR serum or control antibodies that included an isotypic serum and a monoclonal anti-human mitochondrial serum (Chemicon)] in a wet chamber at 4°C. The grids were then washed vigorously with TBS and labeled with AuroProbe (EM GAM IgG, Amersham) for 30 min. Finally, the grids were washed vigorously with water, dried, and examined under the electron microscope (JOEL 1200) at 40 KeV.

RESULTS

Cell Cycle Synchronization. FACS analysis was performed on each of the cell lines after cell cycle synchronization with a double aphidicolin block. The cells were examined after DNA staining with acridine orange, and it was determined that >40% of cells cycled in the manner noted above were in G_2/M

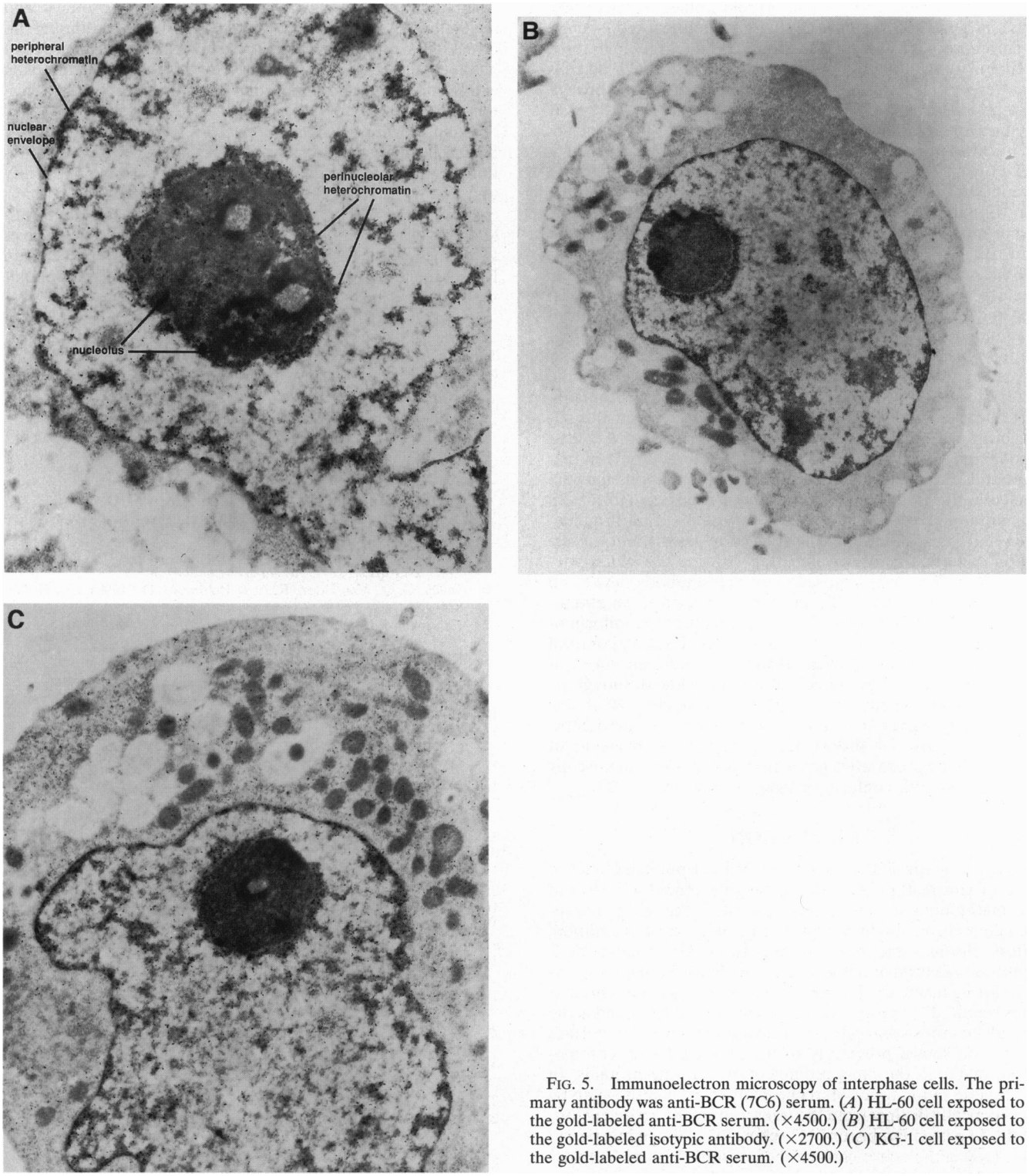

FIG. 5. Immunoelectron microscopy of interphase cells. The primary antibody was anti-BCR (7C6) serum. (*A*) HL-60 cell exposed to the gold-labeled anti-BCR serum. (×4500.) (*B*) HL-60 cell exposed to the gold-labeled isotypic antibody. (×2700.) (*C*) KG-1 cell exposed to the gold-labeled anti-BCR serum. (×4500.)

following release from the aphidicolin block for the length of their S phase (Fig. 1). Cell viability was about 90% (as demonstrated by trypan blue exclusion) during the block and remained unchanged after release. If the cells were released from the block for periods of time longer than their S phase, they gradually returned to the unsynchronized pattern with <10% of cells in G_2/M phase (as reflected by acridine orange staining of DNA content) when the release period was equal to double the S phase.

BCR Associates with Mitotic Chromosomes. As assessed by immunofluorescence and light microscopy, cells in G_0/G_1 showed predominantly cytoplasmic localization of BCR (Fig. 2*A*). In contrast, in cells undergoing mitosis, BCR appeared to line the chromosomal surface (Fig. 2 *C* and *G*). These results were confirmed by using both the monoclonal anti-BCR serum (7C6) (Fig. 2) and the rabbit polyclonal anti-BCR serum (data not shown). Blocking with cognate peptide (Fig. 2 *B* and *E*) and use of an isotypic control antibody (Fig. 2*H*) or preimmune rabbit serum (data not shown) showed no significant labeling. The perichromosomal localization of BCR was further confirmed by swelling the cells with KCl to better visualize the individual mitotic chromosomes (Fig. 2 *G* and *H*). Confocal

laser scanning microscopy (Fig. 3) and immunoelectron microscopy (Fig. 4 *A* and *B*) also demonstrated marked labeling of chromosomes by BCR antisera in cells undergoing mitosis. Predominantly perichromosomal labeling was seen in all cells that were in any of the stages of mitosis from prophase through telophase (Figs. 2–4 and data not shown), regardless of whether or not the cells had been cell cycle-synchronized. Identical results were observed in cell lines of myeloid (HL-60, KG-1) (Figs. 2–4), monocytic (THP-1), and lymphoblastoid (Daudi) lineage (data not shown). Localization studies with a control antimitochondrial antibody showed only cytoplasmic localization regardless of the stage of the cell cycle (data not shown).

BCR Associates with Heterochromatin in Interphase Cells. Further examination of HL-60 (Fig. 5*A*) as well as KG-1 (Fig. 5*C*) and Daudi cells (data not shown) in G_0/G_1 and S phases by immunoelectron microscopy demonstrated that nuclear and cytoplasmic localization of BCR actually occurred throughout the cell cycle. The nuclear material specifically labeled was the heterochromatin, with little-to-no labeling of euchromatin. Heterochromatin labeling was diffuse and included the perinuclear heterochromatin, the heterochromatin distributed throughout the nucleus, and the shell of heterochromatin that surrounds the nucleolar bodies and its invaginations into the nucleolus. Results were the same when the cells were fixed with 2% glutaraldehyde (Figs. 4 and 5) or with 4% paraformaldehyde and 0.1% glutaraldehyde (data not shown), but preservation of ultrastructures was better with the 2% glutaraldehyde. Control samples exposed to isotypic antibody showed no labeling (Figs. 4*C* and 5*B*), and those exposed to an antimitochondrial antibody showed labeling only over the mitochondria (data not shown). Finally, examination of cells by confocal microscopy confirmed nuclear as well as cytoplasmic localization of BCR in interphase cells (data not shown), though by this technique the ratio of cytoplasmic to nuclear BCR was considerably higher than that seen by electron microscopy, perhaps because of differential extraction or masking of antigens in the preparative procedures for electron microscopy as compared with confocal or light microscopy (22, 23).

DISCUSSION

Heterochromatin is the condensed, transcriptionally inactive form of chromatin (24). The very highly condensed form of chromatin found in mitotic chromosomes is thought to resemble heterochromatin in its high degree of packing; in addition, mitotic chromosomes are also transcriptionally inactive. Condensation of chromatin is associated with and perhaps responsible for its inactivity. Furthermore, condensation of chromatin is required for progression through the cell cycle and is the prelude to mitosis and cytokinesis. Although several molecules have been shown previously to be associated with chromosomal material, the most prominent are histone proteins. In this regard, nonmitotic heterochromatin has been shown to be biochemically distinct from the transcriptionally active euchromatin. In particular, histone H1 seems to be less tightly bound to at least some active chromatin, and some histone subtypes appear to be more highly phosphorylated in heterochromatin (25). Serine/threonine phosphorylation of histone H1 is implicated in the control of chromosome condensation (and hence cell cycle progression) (26). This process is mediated by maturation-promoting factor (MPF), which is composed of CDC2 (a key cell cycle regulatory serine/threonine kinase) and a mitotic cyclin (27, 28). CDC2 kinase is itself regulated by phosphorylation-dephosphorylation reactions and by its interaction with cyclins (29). A number of potential substrates for CDC2 in addition to histone H1 have been identified, and they include other proteins that are attached to chromatin [such as the high-mobility-group nonhistone proteins and nucleolin (30–32)] and, interestingly, ABL (33). Although no direct link between BCR and these proteins (other than ABL) has been demonstrated previously, it has been shown that BCR is a serine/threonine kinase that can transphosphorylate histones *in vitro* (12).

The presence of BCR in the nucleus and its association with heterochromatin and mitotic chromosomes necessitates a rethinking of its intracellular function and raises the possibility of a role for BCR in chromosomal condensation and perhaps even in cell cycle control. These observations and the postulated serine/threonine kinase activity of BCR lend themselves to further studies examining potential interactions between BCR, other chromatin-associated proteins, and the phosphokinase network that regulates them.

We thank Michael Underbrink for his excellent technical assistance. This work was supported in part by National Institutes of Health Grant CA-16672.

1. Nowell, P. C. & Hungerford, D. A. (1960) *Science* **132,** 1497.
2. Shtivelman, E., Lifshitz, B., Gale, R. P. & Canaani, E. (1985) *Nature (London)* **315,** 550–554.
3. Kurzrock, R., Gutterman, J. U. & Talpaz, M. (1988) *N. Engl. J. Med.* **319,** 990–997.
4. Kurzrock, R., Shtalrid, M., Romero, P., Kloetzer, W. S., Talpaz, M., Trujillo, J. M., Blick, M., Beran, M. & Gutterman, J. U. (1987) *Nature (London)* **325,** 631–635.
5. Heisterkamp, N. G., Jenster, J., ten Hoeve, J., Zovich, D., Pattengale, P. K. & Groffen, J. (1990) *Nature (London)* **344,** 251–253.
6. Daley, G. Q., Van-Etten, R. A. & Baltimore, D. (1990) *Science* **247,** 824–830.
7. Konopka, J. B., Watanabe, S. M. & Witte, O. N. (1984) *Cell* **37,** 1035–1042.
8. Kloetzer, W., Kurzrock, R., Smith, L., Talpaz, M., Spiller, M., Gutterman, J. U. & Arlinghaus, R. (1985) *Virology* **140,** 230–238.
9. McWhirter, J. R. & Wang, J. Y. (1991) *Mol. Cell. Biol.* **11,** 1553–1565.
10. Arlinghaus, R. B. (1992) *Mol. Carcinogen.* **5,** 171–173.
11. Stam, K., Heisterkamp, N., Reynolds, F. H. & Groffen, J. (1987) *Mol. Cell. Biol.* **7,** 1955–1960.
12. Maru, Y. & Witte, O. N. (1991) *Cell* **67,** 459–468.
13. Adams, J. M., Houston, H., Allen, J., Lints, T. & Harvey, R. (1992) *Oncogene* **7,** 611–618.
14. Ron, D., Zannini, M., Levis, M., Wickner, R. B., Hunt, L. T., Graziani, G., Tronick, S. R., Aaronson, S. A. & Eva, A. (1991) *New Biol.* **3,** 372–379.
15. Ridley, A. J., Self, A. J., Kasmi, F., Paterson, H. F., Hall, A., Marshall, C. J. & Ellis, C. (1993) *EMBO J.* **12,** 5151–5160.
16. Hall, A. (1992) *Cell* **69,** 389–391.
17. Diekmann, D., Brill, S., Garrett, M. D., Totty, N., Hsuan, J., Monfries, C., Hall, C., Lim, L. & Hall, A. (1991) *Nature (London)* **351,** 400–402.
18. Dhut, S., Dorey, E. L., Horton, M. A., Ganesan, T. S. & Young, B. D. (1988) *Oncogene* **3,** 561–566.
19. Wetzler, M., Talpaz, M., Van Etten, R. A., Hirsh-Ginsberg, C., Beran, M. & Kurzrock, R. (1993) *J. Clin. Invest.* **92,** 1925–1939.
20. Heintz, N., Sive, H. & Roeder, R. G. (1983) *Mol. Cell. Biol.* **3,** 539–550.
21. Ben-Neriah, Y., Daley, G. Q., Mes-Masson, A.-M., Witte, O. N. & Baltimore, D. (1986) *Science* **233,** 212–214.
22. Melan, M. A. & Sluder, G. (1992) *J. Cell Sci.* **101,** 731–743.
23. Bendayan, M., Nanci, A. & Kan, F. W. K. (1987) *J. Histochem. Cytochem.* **35,** 983–996.
24. Brown, S. W. (1966) *Science* **151,** 417–425.
25. Bradbury, E. M. (1992) *Bioassay* **14,** 9–16.
26. Matsumoto, P., Yasuda, H., Mita, S., Marunouchi, T. & Yamada, M. (1980) *Nature (London)* **284,** 181–183.
27. Arion, D., Meijer, L., Brizuela, L. & Beach, D. (1988) *Cell* **55,** 371–378.
28. Labbe, J. C., Picard, A., Peaucellier, G., Cavadore, J. C., Nurse, P. & Doree, M. (1989) *Cell* **57,** 253–263.
29. Fleig, U. N. & Gould, K. L. (1991) *Semin. Cell Biol.* **2,** 195–204.
30. Reeves, R., Langan, T. A. & Nissen, M. S. (1991) *Proc. Natl. Acad. Sci. USA* **88,** 1671–1675.
31. Belenguer, P., Caizergues-Ferrer, M., Labbe, J. C., Doree, M. & Amalric, F. (1990) *Mol. Cell. Biol.* **10,** 3607–3618.
32. Nigg, E. A. (1991) *Semin. Cell Biol.* **2,** 261–270.
33. Kipreos, E. T. & Wang, J. Y. J. (1990) *Science* **248,** 217–220.